Selection for infectivity profiles in slow and fast epidemics, and the rise of SARS-CoV-2 variants

François Blanquart[1], Nathanaël Hozé[2], Benjamin J. Cowling[3,4], Florence Débarre[5], Simon Cauchemez[2]

1. Centre for Interdisciplinary Research in Biology (CIRB), Collège de France, CNRS, INSERM, PSL Research University, Paris, France
2. Mathematical Modelling of Infectious Diseases Unit, Institut Pasteur, Université de Paris, UMR2000, CNRS, Paris, France
3. WHO Collaborating Centre for Infectious Disease Epidemiology and Control, School of Public Health, Li Ka Shing Faculty of Medicine, The University of Hong Kong, Pokfulam, Hong Kong Special Administrative Region, China
4. Laboratory of Data Discovery for Health, Hong Kong Science and Technology Park, New Territories, Hong Kong Special Administrative Region, China
5. Institute of Ecology and Environmental Sciences of Paris (iEES-Paris, UMR 7618), CNRS, Sorbonne Université, UPEC, IRD, INRAE, 75252 Paris, France

Abstract

Evaluating the characteristics of emerging SARS-CoV-2 variants of concern is essential to inform pandemic risk assessment. A variant may grow faster if it produces a larger number of secondary infections (transmissibility advantage) or if the timing of secondary infections (generation time) is better. So far, assessments have largely focused on deriving the transmissibility advantage assuming the generation time was unchanged. Yet, knowledge of both is needed to anticipate impact. Here we develop an analytical framework to investigate the contribution of both the transmissibility advantage and generation time to the growth advantage of a variant. We find that the growth advantage depends on the epidemiological context (level of epidemic control). More specifically, variants conferring earlier transmission are more strongly favoured when the historical strains have fast epidemic growth, while variants conferring later transmission are more strongly favoured when historical strains have slow or negative growth. We develop these conceptual insights into a statistical framework to infer both the transmissibility advantage and generation time of a variant. On simulated data, our framework correctly estimates both parameters when it covers time periods characterized by different epidemiological contexts. Applied to data for the Alpha and Delta variants in England and in Europe, we find that Alpha confers a +54% [95% CI, 45-63%] transmissibility advantage compared to previous strains, and Delta +140% [98-182%] compared to Alpha, and mean generation times are similar to historical strains for both variants. This work helps interpret variant frequency and will strengthen risk assessment for future variants of concern.

Introduction

Human pathogens rapidly adapt to their hosts. During the short evolutionary history of SARS-CoV-2 with humans, since the host shift in late 2019, several selected mutations and combinations of mutations (variants) have emerged: for example, the D614G mutation in Spring 2020 (1), the variant Alpha in Fall 2020 (B.1.1.7), and Delta in Spring 2020 (B.1.617.2). Variant Alpha, first detected in England in September 2020, rapidly rose in frequency in October 2020 in England and spread to multiple countries, causing important rebounds of the epidemic (2–6). Since then, the Delta variant has become dominant in many parts of the world, leading to new surges in infections and hospitalisations.

Each time a variant of concern emerges, it is essential to determine whether it has acquired a competitive advantage compared to circulating SARS-CoV-2 strains, in order to anticipate the potential effects on the epidemic trajectory and hospital admissions. The advantage can be caused by an increased capacity to transmit or to escape the immune response acquired by previous infection or vaccination. The *transmissibility advantage* of an emerging variant has been defined as the relative increase in the effective reproduction number R (average number of secondary cases). It has often been estimated by analysing the rise in the variant's frequency, under the assumption that all strains shared the same generation time (GT) distribution (i.e. delay between infection in the primary case and the people they infect). However, this has sometimes led to unstable estimates of the transmissibility advantage. For example, in the United Kingdom, the transmissibility advantage of the Alpha variant was estimated to decline from +89% to +54% from December to mid-January. Estimates of transmissibility advantage of Alpha and Delta across countries also exhibit substantial variability (7). The reasons why estimates of the transmissibility advantage would vary with the epidemiological context remain obscure. The instability this generates is problematic for planning since it affects medium and long-term evaluations of the epidemic trajectory. It also suggests that methods currently used to ascertain the risks posed by emerging variants may miss important drivers of emergence.

The evolutionary fate of the variant is ultimately determined by its exponential growth rate relative to that of the circulating strains. When evaluating the growth advantage of a variant, the focus has so far largely been on estimating differences in R. However, the growth rate of an emerging variant depends not only on the effective reproduction number but also on the generation time (GT) distribution. Natural selection is therefore expected to act on the full infectivity profile, which combines both R and GT. Here we develop a mathematical model to

investigate how the growth advantage may vary with the epidemiological context when variants have different generation times. We use the relationship between infectivity profile and growth rate to explore conceptually how infectivity profiles are selected for. We find that the growth advantage of a variant generally depends on the epidemiological context, more precisely on whether transmission is low (declining or slow epidemic) or high (fast epidemic). We call transmission the rate of infectious contacts in the community, which depends on the epidemiological context, for example social distancing, mask-wearing, population immunity, seasonal effects, etc. We use the time-varying reproduction number of the historical strain (taken as a reference), denoted $R_H(t)$, as a proxy for transmission. Our conceptual exploration suggests that it is possible to infer changes in infectivity profile associated with an emerging variant, and not only its growth rate, in settings where transmission changes over time. We thus develop an inference framework to estimate changes in infectivity profile associated with a variant and more precisely characterize the transmissibility advantage of the variant and its dependency to the epidemiological context. We apply our approach to data on Alpha and Delta variants frequency over time in England in Fall 2020 and Spring 2021.

Results

General principle

We consider a situation where a variant, or a set of strains with similar properties, have been circulating for some time (historical strains *H*) and is challenged by an emerging variant *E*. When investigating the rise of variant *E* relative to historical strains *H*, we typically only observe the exponential growth rates of *H* and *E* strains, which translates into a growth advantage (or disadvantage). More precisely, if the historical strains grow with exponential rate r_H and the emerging variant grows with rate r_E, the logit of the frequency of the emerging variant will grow linearly with slope $r_E - r_H$. This slope is called the growth advantage or selection coefficient. The selection coefficient of the emerging variant relative to historical strains is obtained by a linear regression of the logit frequency of the variant over time. It is then typically assumed that both variant and historical strains share the same distribution of generation time. The effective reproduction number of the emerging variant relative to historical strains, called the transmissibility advantage ($R_E/R_H - 1$), can thus be deduced.

Yet natural selection acts on the full infectivity profile of a strain, not only on the effective reproduction number. The infectivity profile is a function $\beta(\tau) = R\, w(\tau)$ of the time since

infection τ, where R is the effective reproduction number, while $w(\tau)$ characterizes the distribution of generation time and satisfies $\int_{\tau=0}^{\infty} w(\tau)d\tau = 1$.

Selection for infectivity profiles in slow and fast epidemics

We first examine how the selection coefficient $r_E - r_H$ varies with transmission for various infectivity profiles of the variant compared to historical strains (Figure 1). To do so, we use a formula relating the growth rate to the effective reproduction number and the distribution of the generation time (Methods). This formula assumes that each variant grows or declines exponentially and that the distribution of the time since infection is at any time at its equilibrium value: an exponential distribution with rate equal to the exponential growth rate (8). This equilibrium distribution naturally follows from the assumption of exponential growth, which implies that individuals infected $t + \Delta t$ days ago are $e^{r\,\Delta t}$ more numerous than individuals infected t days ago, with r is the exponential growth rate.

Several scenarios for the emerging variant are considered. We first consider variants with the same effective reproduction number as historical strains, which can be selected for if secondary infections occur at different timings (Figure 1 A, C). A variant with a shorter mean generation time is selected in a growing epidemic because it produces the same number of secondary infections in a shorter time, while the same variant is counter-selected in a declining epidemic (Figure 1C). The opposite holds for variants with a longer mean generation time. A variant with larger standard deviation (sd) in generation time is always selected for because it enjoys both an excess of early secondary infections and late secondary infections compared to historical strains. The opposite holds for a variant with smaller sd in generation time. Generally, in a growing epidemic, more individuals have been infected recently and there is a greater advantage to early transmission, while in a declining epidemic, more individuals have late time since infection and therefore strains that transmit at later times have a greater advantage. Again, this is a direct demographic consequence of growth or decline of the epidemic. Selected variants could thus enjoy a more favourable timing of secondary infections, not a transmissibility advantage (9).

Additionally, an advantage in the timing of secondary infections can of course be combined with a transmissibility advantage. We therefore consider hypothetical emerging variants with a range of generation time distributions and a +10% transmissibility advantage (Figure 1B, D). These variants generally have a stronger growth advantage, but the variation in selection

coefficient with transmission is similar to that of the analogous variants without the transmissibility advantage (Figure 1C, D).

Notably, in both cases there is a level of transmission (R_H) at which all variants perform similarly regardless of their distribution of generation time. This level of transmission is precisely where the size of the variant epidemic is constant in time (variant growth rate is 0). For example, this level of transmission is $R_H = 1$ for a variant not affecting transmissibility (Figure 1C). For a 10% transmissibility advantage, this level is $R_H = 1/1.1$ (Figure 1D). Generally, for a variant conferring a transmissibility advantage s_1, the level of transmission is $R_H = 1/(1 + s_1)$. At this level of transmission, the distribution of time since infection is uniform—all ages of infection are equally represented—and therefore the infectivity profile does not matter for selection on the variant.

While these results assume that the time since infection is fixed at its equilibrium distribution, it is not necessarily the case in a realistic scenario where transmission changes over time. We applied these analytical results to simulations where the time since infection structure emerges from the model dynamics. The epidemiological dynamics are simulated with discrete-time renewal equations including time-varying transmission, the build-up of population immunity (assumed to be identical for historical strains and emerging variant), and detection and isolation of cases (Methods). In the context of progressive control of an epidemic, variants with the same reproduction number but distinct generation time distributions can exhibit a variety of epidemiological and frequency dynamics (Figure 2A, C). The epidemiological dynamics, that is the daily number of variant cases, are also strongly affected by the generation time distribution of the variant (Figure 2A). Frequency trajectories can be non-monotonous: a variant with shorter mean generation time could be selected, increase in frequency, but then decline in frequency as the epidemic is controlled (Figure 2C). Several variants all sharing the same 10% transmissibility advantage exhibit a range of frequency trajectories in the simulations: the trajectories of one of them resemble that of a variant with a +30% advantage and same generation time distribution as historical strains (Figure 2D, light blue line compared to +30% curve), while others stagnate at low frequency (Figure 2D, blue and green lines).

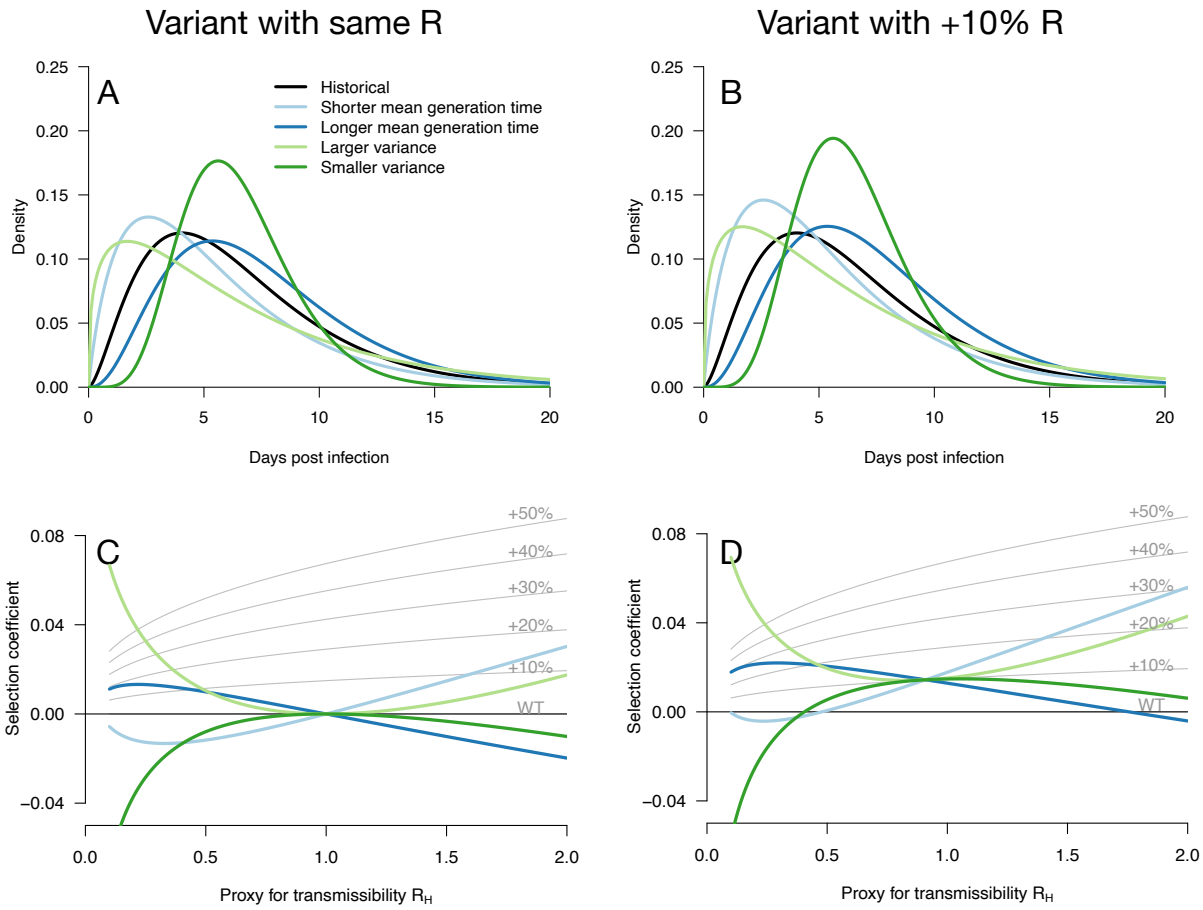

Figure 1: Variation of the selection coefficient as a function of transmission, for several infectivity profiles of emerging variants. Panels A, B show several variant infectivity profiles with the same effective reproduction number as historical strains (A) or an effective reproduction number increased by +10% (B). For variants with shorter or longer mean generation time, the relative mean generation time is -15% or +15% compared to historical strains. For variants with shorter or longer sd in generation time, the relative sd in generation time is -40% or +40% compared to historical strains. The Panels C, D show for these variants, the selection coefficient as a function of the proxy for transmission (effective reproduction number of the historical strains). The gray lines show the selection coefficient if the variant had the same infectivity profile as historical strains, only increased uniformly by a constant as commonly assumed.

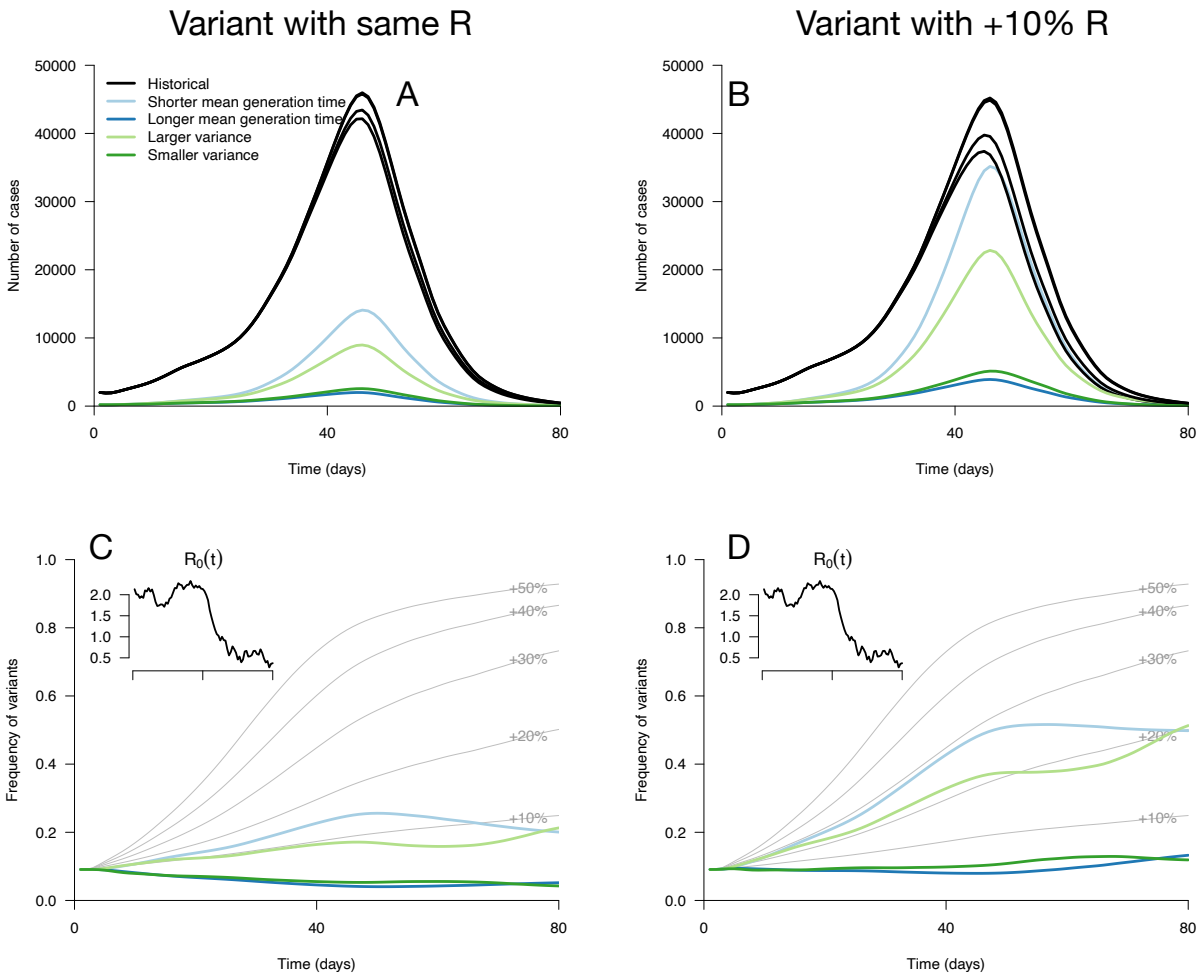

Figure 2: Epidemiological and evolutionary trajectories of several types of emerging variants competing with historical strains. Panels A, B show epidemiological dynamics (daily cases number of historical strains in black, of variants in colours). Historical strains display several slightly different curves when competing with each of the variants because of the weak competition brought about by the build-up of population immunity. Panels C, D, show evolutionary trajectories, with daily variant frequency as coloured lines. The light gray curves show the frequency dynamics of variants with a +10% to +50% transmissibility advantage, with the same generation time as historical strains. The inset shows the transmission through time in these simulations, given by the basic reproduction number of historical strains (see details of simulation model in Methods).

Inference of the infectivity profiles of variants

The variety of variant trajectories shown on Figure 2 suggests that it may be possible to infer the changes in infectivity profiles of variants by analysing their growth advantage as a function of transmission when we have accumulated sufficient data documenting growth rates in different epidemiological situations. We first tested this idea on simulated data, in scenarios of emergence and progressive control of the variant.

Our inference framework is based on the relationship between growth rates of historical strains (r_H) and of the emerging variant (r_E). Our aim is to infer three parameters s_1, s_2, s_3, characterizing respectively the transmissibility advantage, the mean generation time and the sd of generation time of the emerging strain relative to that of historical strains. The relationship can be used to infer properties of the variant infectivity profile, but not with a classical linear regression because both r_H and r_E are measured with errors with a complex covariance structure. Furthermore, large errors can blur the subtle distinction between different profiles (Supplementary Figure 1). The error variance is inversely related to the number of cases and the size of the sample used to assay variant frequency ("sample size"). When the total number of cases and the sample size are both large, the joint distribution of the time series of estimated $\hat{r}_H$ and $\hat{r}_E$ is approximately multivariate normal (Methods). The mean vector of the multivariate normal depends on the parameters $R_H(t)$ (the time series of effective reproduction number), of the mean and sd of the historical strains' generation time (fixed to 6.5 and 4 days), and of the parameters of interest s_1, s_2, s_3. The variance-covariance structure of the multivariate normal distribution is fixed and depends on the daily total number of cases and the sample size. It is also possible to derive the multivariate normal distribution of $\hat{r}_H$ and $\hat{r}_E$ across different independent regions instead of over time (Methods).

With this statistical framework at hand, we conducted a simulation study to infer jointly the transmissibility advantage of the variants and their relative mean generation time (Figure 3). In these simulations, we systematically varied the infectivity profile of the emerging strain: transmissibility advantage (s_1) from +0 to +50% and relative mean generation time (s_2) from -40% to +40%. We assumed the emerging strain had the same sd of generation time as historical strains ($s_3 = 0$). We jointly inferred the two parameters s_1 and s_2 for different sample sizes (sample size, N = 1000, 3000, 10000 per day) and for different scenarios of variability in epidemiological context, from a strong to a weak decline. In the explicit simulations, the parameter that we tune is the *basic* reproductive number $R_{0,H}(t)$ assumed to decline from 1.5 to 0.5, 1.3 to 0.7 and 1.1 to 0.9 over 80 days in the three scenarios, and the inferred parameters represent the *effective* reproductive number after accounting for population immunity and case detection and isolation (Supplementary Figure 2).

The transmissibility advantage was almost always precisely inferred even with small sample size and small variability in effective reproduction number (Figure 3, left panels). In contrast, the relative mean generation time was well inferred only for a large sample size and large variability in effective reproduction number (Figure 3, right panel). This was because the large

error on r_E and r_H due to the limited sample size, in conjunction with the small variability in $R_{0,H}(t)$ makes precise inference of the relationship between r_E and r_H difficult. For such small sample sizes, grouping data by week (instead of by days, for the same duration) improves inference (Figure 3, green points).

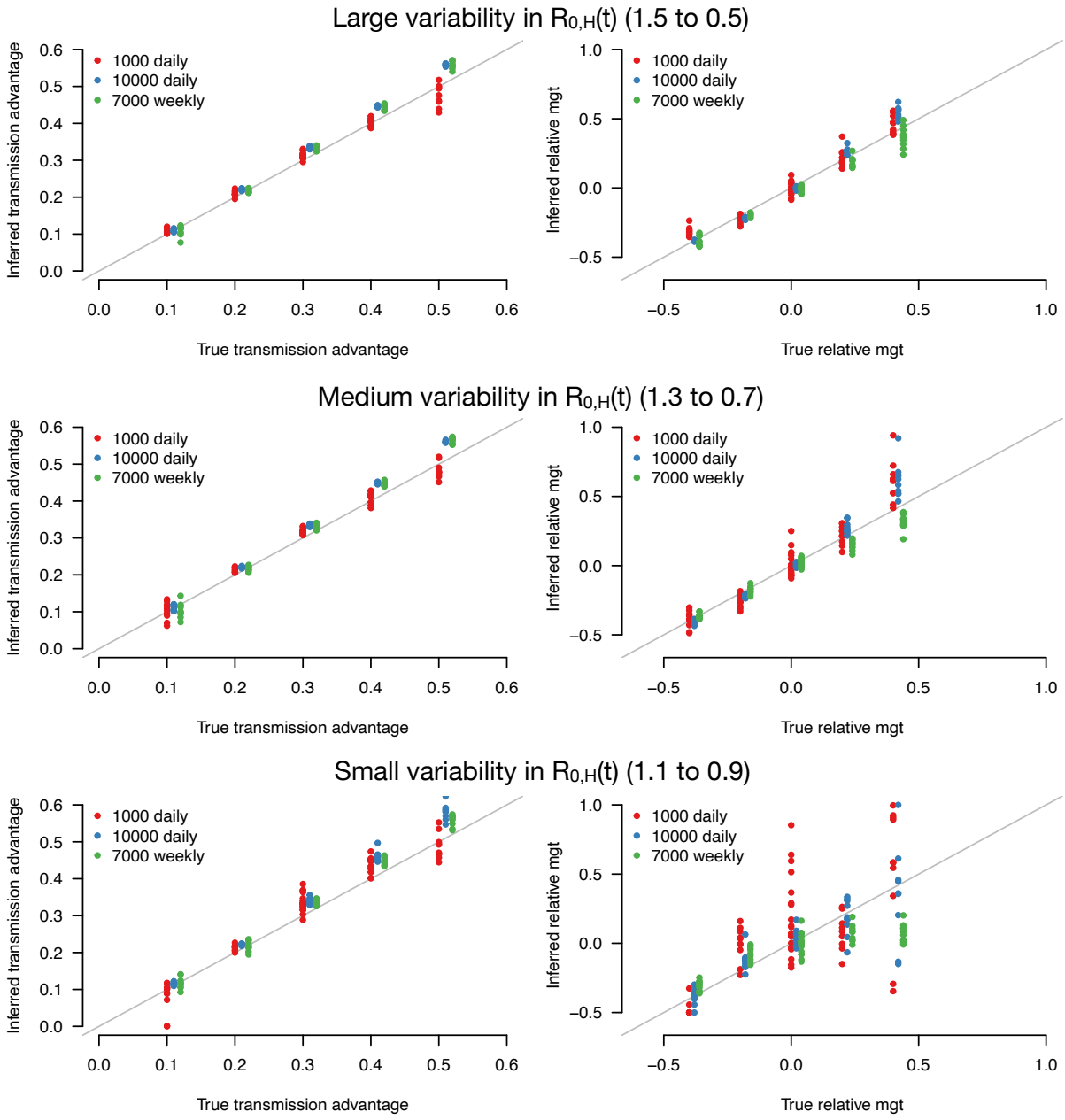

Figure 3: Inference of the transmissibility advantage and relative mean generation time in the simulation study. The plots show the correlation between inferred and true quantities. The three colours show different sample sizes used to infer variant frequency: 1000 daily, 10000 daily, and 1000 daily grouped by week (7,000 weekly). The left panels show the transmissibility advantage, the right panels the mean generation time (mgt). Top, middle and bottom panels show inference for large, medium and small variability in $R_{0,H}(t)$. The simulations are initialized with $I_H(0,0) = 4000$ and $I_E(0,0) = 80$. For the inference of the transmissibility advantage we used a variant relative mean generation time of $s_2 = +0\%$ (also inferred by the model), while for the inference of relative mean

generation time we used a variant transmissibility advantage of $s_1 = +30\%$ or $s_1 = +45\%$ (for relative mean generation time $s_2 = +20\%$ and $s_2 = +40\%$). For each parameter combination, 10 replicate simulations were drawn with the same parameters, hence the same deterministic epidemiological dynamics, but with different random error on data (Poisson error on cases number and binomial error on frequencies).

Application to the variants Alpha and Delta in England

We used this framework to infer the transmissibility advantage and mean generation time of Alpha (B.1.1.7) in England. We used public data from Public Health England on weekly cases numbers and frequency of the Alpha variant (dataset 1). In England, the frequency of the Alpha variant could be quickly inferred because some of the PCR tests for SARS-CoV-2 detection presented a "S gene target failure" (SGTF) caused by the spike 69/70 deletion characteristic of Alpha (10). The variant Alpha swept through from 0% to almost 100% frequency over 25 weeks; data were of very good quality for the whole period (Figure 4). Using our framework, we found that Alpha had a transmissibility advantage equal to $s_1 = 54\%\ [45, 63\%]$, and the same mean generation time as previous strains, $s_2 = 0.058\ [-0.095, 0.21]$ (Figure 5).

We next evaluated the growth of Delta (B.1.617.2) in England. As Delta does not have the spike 69/70 deletion, the growth of Delta and eventual replacement of Alpha in April and May 2021 was evidenced by the decline of SGTF (11) (dataset 2). However, we found that with this temporal data, we could not reliably disentangle the transmissibility advantage from the mean generation time. The confidence intervals were very wide, with an estimated transmissibility advantage equal to $s_1 = 229\%\ [7, 451\%]$ and a mean generation time estimated at $s_2 = 1\ [-0.31, 2.3]$. This was linked to the small temporal variations in epidemic conditions in this short period of time compared to the previous period when we investigated Alpha (Supplementary Figure 3).

In an attempt to gain more power to disentangle the transmissibility advantage from the mean generation time for the Delta variant, we used *spatial* variation in growth rates across European countries. We used data from the European Surveillance System (TESSy) on the growth rate of "historical" strains circulating at the time when Delta emerged (mainly Alpha variant), and the emerging Delta variant across 11 European countries with sufficient genomic data (Austria, Belgium, Denmark, France, Germany, Greece, Ireland, Italy, Netherlands, Norway, Sweden: dataset 3). With these data, we inferred a transmissibility advantage equal to $s_1 = 140\%\ [98, 182\%]$ compared to Alpha, and a mean generation time similar to the Alpha variant at $s_2 = 0.033\ [-0.18,\ 0.25]$.

In conclusion, we found that the Alpha variant had a transmissibility advantage of +54% compared to historical strains, and the Delta variant had a further transmissibility advantage of +140% relative to Alpha, assuming a mean generation time of 6.5 days. There was no evidence of an altered mean generation time for these two variants. Intuitive patterns in the inferred relationship testify from the fact that Alpha and Delta have (Figure 5): the relation between growth rates r_E and r_H runs almost parallel to the bisector, indicating that the selection coefficient does not change much with epidemiological conditions. The analytical relationship between r_E and r_H would imply on the contrary a steeper slope for a variant shortening the mean generation time, and a flatter slope for a variant prolonging the mean generation time (Methods, Figure 5A, Supplementary Figure 1).

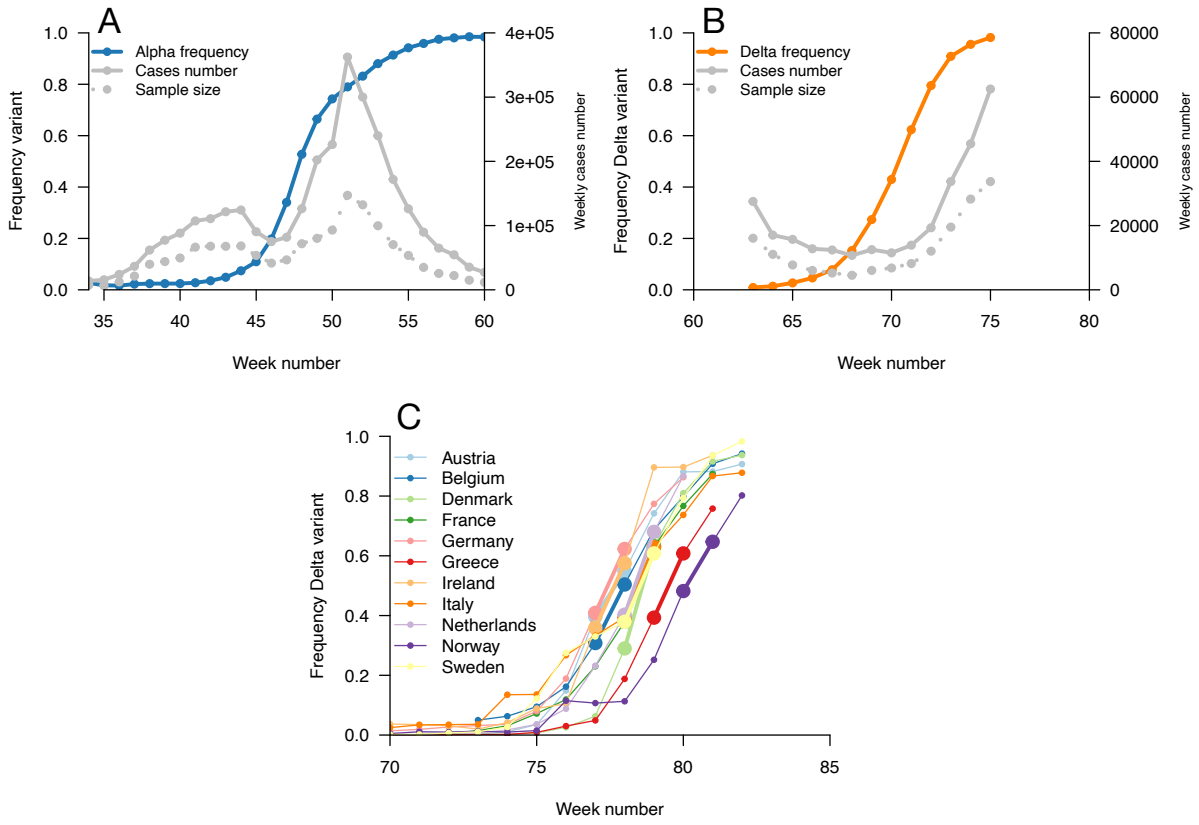

Figure 4: Data used for inference. Top panels, dynamics of the Alpha variant frequency in England (left) and of the Delta variant frequency in England (right), estimated through SGTF. These frequencies are shown together with the dynamics of weekly cases numbers, over weeks 35 (week starting 08/09/2020) to 60 (week starting 02/03/2021) for Alpha, and weeks 63 (starting 23/03/2021) to 75 (starting 15/06/2021) for Delta. Bottom panel,

the dynamics of the Delta variant frequency in 11 chosen European countries. For each country we used the growth rate of historical strains and emerging Delta variant when the frequency passes 50%, highlighted with larger points and thicker line on the figure.

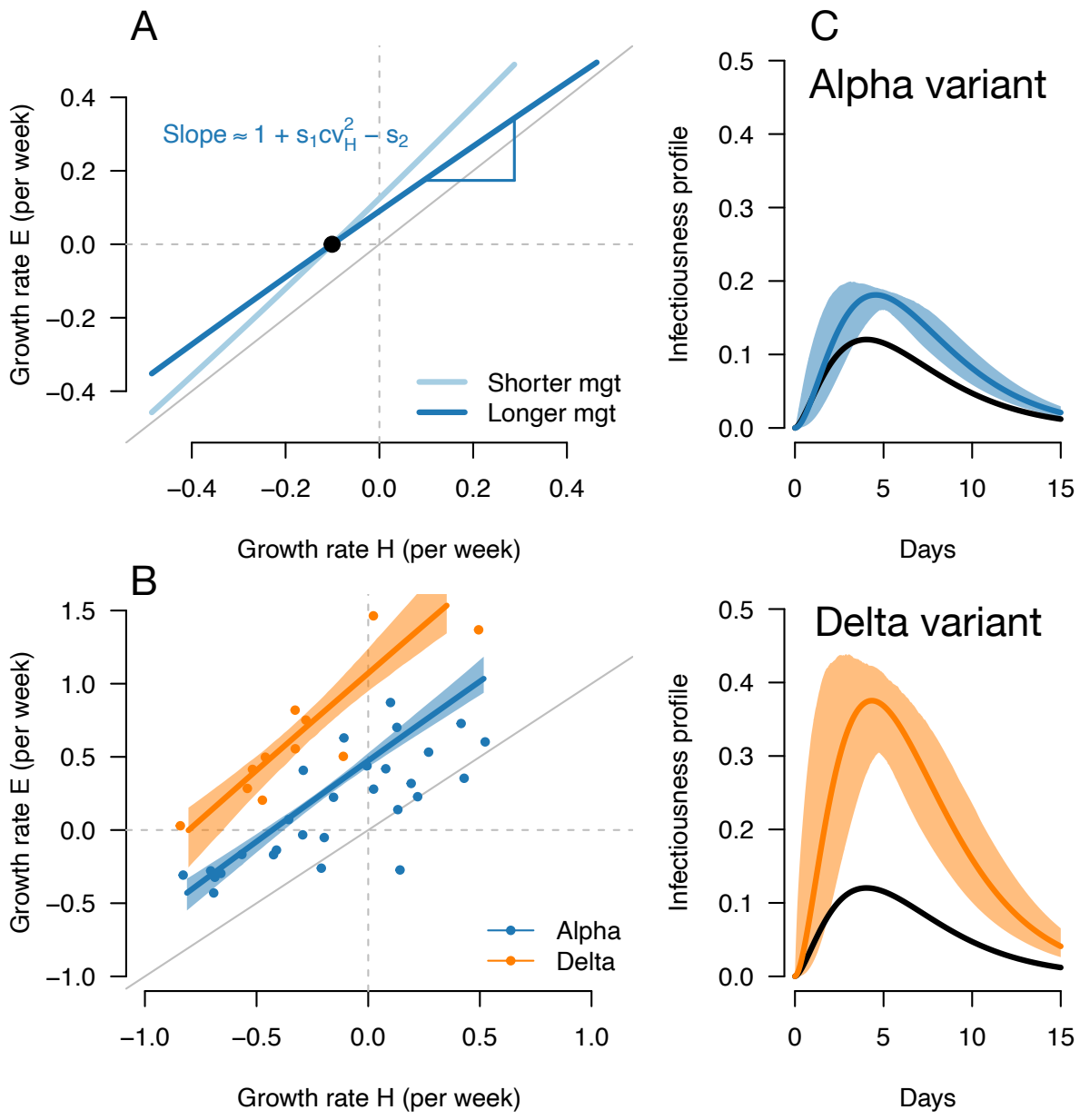

Figure 5: A, Geometric intuition for how the (r_H, r_E) relationship depends on the mean generation time for hypothetical variants with transmissibility advantage $s_1 = 0.1$ and relative mean generation time of $s_2 = -0.15$ and $s_2 = +0.15$ (as in Fig. 1, 2). B, the correlation between estimated growth rates of historical strains and variant in England. For Alpha (dataset 1) this is a temporal correlation in England over weeks starting 08/09/2020 to 16/03/2021. For Delta (dataset 3) this is a *spatial* correlation across European countries. The curves with confidence intervals are the model fits for each variant and show that the selection coefficient (the vertical distance to the bisector) is roughly constant across epidemiological conditions, indicative that the mean generation time is

not altered in these variants. C, the inferred infectivity profile of each variant with confidence intervals, together with the infectivity profile of historical strains circulating before the rise of the Alpha variant (black curve).

Discussion

We investigated how emerging variants with distinct infectivity profiles may be selected. Our main finding is that levels of transmission reflected in the reproduction number *R(t)*, which depend on human behaviour and interventions, change selection on different types of variants. In a context of high transmission and high growth rate ("fast" epidemic), most infections will be recent and it is more advantageous to transmit early. Conversely, in a context of low transmission ("slow" or declining epidemic), infections will be older and it is more advantageous to transmit late. The selection coefficient on variants may thus increase or decrease with transmission, and it can even be a non-monotonous function of transmission. A second important finding is the variation of the selection coefficient with transmission provides insight on the infectivity profile. We used this understanding to infer variant infectivity profiles from the variation in growth rates in contexts of changing transmission.

We found that Alpha variants enjoy a transmissibility advantage of +54% [45, 63] relative to historical strains, and Delta variants a +140% [98, 182] additional advantage relative to Alpha. Both variants have a mean generation time similar to that of historical strains (here assumed to be 6.5 days). This complements previous findings: the possibility of a shorter generation time was investigated to explain the growth advantage of Alpha, but previous studies found it was difficult to distinguish a variant with larger transmissibility from one with a shorter generation time (2,3). Some (but not all) studies of within-host viral load dynamics suggested that individuals infected by variant Alpha could shed virus for a longer time, which may result in a longer generation time (12–14). Conflicting results exist for Delta. A cluster of Delta variant infections in China suggested a smaller mean generation time (2.9 days) and more pre-symptomatic transmission for Delta than early SARS-CoV-2 strains, but without good control (15); more controlled studies found on the contrary a similar generation time (16,17). If the distribution of generation time is similar in Delta as we infer, the observed growth rates imply it is +140% more transmissible than Alpha, in line with the +70 to +200% estimated elsewhere (18,19). If the generation time of Delta had instead been inferred 1 or 2 days shorter than the baseline (6.5 days), the observed growth rate would imply the estimated transmissibility

advantage drops to +106% or +77%. The large transmissibility advantage of Delta with similar mean generation time makes it more difficult to control with interventions reducing transmission (such as social distancing) than if it had a smaller transmissibility advantage associated with a shorter mean generation time.

Our conceptual results may be useful to interpret the dynamics of variant frequency dynamics. Frequency dynamics are determined by the selection coefficient, which is the difference in growth rates between the variant and historical strains. Several papers have reported a varying selection coefficient across time (20) or across countries (7). One possible explanation for this variability is that the selection coefficient changes with transmission because of differences in generation time distributions, which may explain non-monotonous frequency trajectories (Figure 2C).

Evolution influences epidemiological dynamics: at a given level of transmission, stronger selection on a variant also implies a larger incidence of the variant and therefore a larger burden on healthcare systems (Figure 2A). However, we emphasize that measures to reduce transmission, although possibly increasing the *selection coefficient*, always result in reduced variant *absolute growth rate* and better control of the variant. Indeed, it remains true that a variant epidemic growth rate is an increasing function of transmission, and a variant is growing if and only if $R_E > 1$ (Equation 3).

A limitation of our framework is that we only consider the impact of changing transmission on selection for variants. We do not consider the impact of interventions shortening the distribution of generation time such as isolation of positive cases and contact tracing, which also potentially change over time (21). These interventions would alter the selection coefficient differently, in particular would favour earlier transmission (shorter mean generation time). We do not consider either the impact of other changes in the environment. For example, the positive selection on vaccine escape variants may increase over time in the context of rapid vaccination of the population. Analogously, different levels of vaccination across countries could also affect the spatial analysis of spread of a vaccine escape variant. Lastly, we consider only one emerging variant. Our inference framework could readily be extended without additional technical complications to the frequency dynamics of several variants. In spite of these limitations, our simple framework makes minimal assumptions (exponential growth rate and stable age-of-infection structure) that proved robust when tested against a simulation model including more complicated features (build-up of immunity, isolation of positive cases, explicit epidemiological dynamics in the context of changing transmission).

In conclusion, we developed a conceptual framework to study selection on variants modifying the transmission of an infectious pathogen. We decoupled selection on transmissibility (number of secondary infections) and selection on the distribution of generation time (timing of secondary infections). While selection on number of secondary infections is stronger with increased transmission (e.g., contact rates) in the community, selection on the generation time varies with levels of transmission in the community. This can lead to non-monotonous variant frequency trajectories. The ensuing variation in the selection coefficient in contexts of changing transmission can be used to infer not only the transmissibility advantage of variants, but also the change in mean generation time. This inference method could be used in conjunction with other type of data, for example data on variant viral load trajectories (13,22), or comparison of secondary attack rates of variant vs. historical strains informing on the transmissibility advantage (23). We find that the patterns of growth of the Alpha and Delta variants in England and in Europe are compatible with mean generation times similar to historical strains. This work will help understand variant dynamics at a time when several variants of concern are circulating and new ones may evolve, and genomic and PCR-based surveillance programs allow fine monitoring of their dynamics.

Methods

The model

Relationship between growth rate and effective reproduction number

We describe the exponential growth of an epidemic within a simple framework. We assume that transmission changes over time because of varying social distancing measures. We assume that changes are sufficiently slow compared to the mean generation time that the distribution of time since infection is always at equilibrium. It is known that when the number of infected individuals grows exponentially at a constant rate r, the distribution of time since infection equilibrates to an exponential distribution with parameter r (8). Here we assume that the number of infected individuals grows exponentially with rate $r(t)$ and that the time since infection is exponential with parameter $r(t)$ (i.e., the distribution equilibrates instantaneously when $r(t)$ changes). The timing of infections is defined by the probability density $w(\tau)$. Under these assumptions, the effective reproduction number $R(t)$ reflecting transmission and the growth rate $r(t)$ are linked through (8):

$$r(t) = \int_0^\infty \underbrace{r(t)\, e^{-r(t)\,\tau}}_{\substack{\text{stable age}\\ \text{structure}}} \underbrace{w(\tau)\, R(t)}_{\substack{\text{new infections}\\ \text{from individuals}\\ \text{of age } \tau}} d\tau. \qquad (1a)$$

The growth rate is the integral over all possible times since infection of the probability that an individual has this age (the exponential distribution), times the number of new infections produced by an individual this age, giving the relation (1a). This equation simplifies to:

$$1 = R(t) \int_0^\infty e^{-r(t)\,\tau}\, w(\tau)\, d\tau. \qquad (1b)$$

For a gamma-distributed generation time (with shape and scale parameters α and β), this integral has an explicit solution:

$$R(t) = \left(1 + \beta\, r(t)\right)^{\alpha}. \qquad (2)$$

Conversely, the growth rate is:

$$r(t) = \left(R(t)^{\frac{1}{\alpha}} - 1\right) / \beta. \qquad (3)$$

The epidemic grows when $R(t) > 1$ and declines when $R(t) < 1$. Reparameterising in terms of the mean and standard deviation of the gamma distribution, $\mu = \alpha\, \beta$ and $\sigma = \sqrt{\alpha}\, \beta$, yields:

$$r(t) = (R(t)^{\sigma^2/\mu^2} - 1)(\mu/\sigma^2). \quad (4)$$

Relationship between growth rates of historical strains and emerging variant across epidemiological conditions

This equation can separately describe the growth of historical strains and variants characterized by their own parameters: $R_H(t)$, μ_H and σ_H for historical strains, $R_E(t)$, μ_E and σ_E for the emerging variant. We may recast the variant parameters in terms of how they are altered compared to historical strains:

$$R_E(t) = R_H(t)(1 + s_1), \quad (5)$$

$$\mu_E = \mu_H(1 + s_2),$$

$$\sigma_E = \sigma_H(1 + s_3).$$

We assume that changes in behaviour and in interventions cause temporal variability in the transmission, measured by the effective reproduction number of historical strains taken as the reference, $R_H(t)$, and only in this parameter. This assumption is valid for interventions that reduce transmission (social distancing, vaccines) but not for interventions that change the distribution of generation time (contact tracing, case isolation). Temporal variability in $R_H(t)$ will affect both $r_H(t)$ and $r_E(t)$ through the relationship (4):

$$r_H(t) = \left(R_H(t)^{\frac{\sigma_H^2}{\mu_H^2}} - 1\right)(\mu_H/\sigma_H^2) \quad (6)$$

$$r_E(t) = \left(R_E(t)^{\frac{\sigma_E^2}{\mu_E{}^2}} - 1\right)(\mu_E/\sigma_E^2) = \left(R_H(t)^{\frac{\sigma_E^2}{\mu_E{}^2}}(1 + s_1)^{\frac{\sigma_E^2}{\mu_E{}^2}} - 1\right)(\mu_E/\sigma_E^2)$$

The temporal variation in $R_H(t)$ thus defines a parametric relationship between $r_H(R_H(t))$ and $r_E(R_H(t))$ that can be used to infer s_1, s_2 and s_3. The variation of the selection coefficient with $R_H(t)$ is simply given by $r_E(t) - r_H(t)$.

Approximation of the parametric relationship

To gain further intuition on the parametric relationship between $r_H(R_H(t))$ and $r_E(R_H(t))$ as $R_H(t)$ varies, we compute the tangent of the curve at the value $R_H(t) = 1$ (where r_H is 0). The parameters of this tangent will of course be most informative when values of $R_H(t)$ are not too far from 1. The intercept is:

$$intercept = r_E(1) = \left((1+s_1)^{\frac{\sigma_E^2}{\mu_E{}^2}} - 1\right)(\mu_E/\sigma_E^2) \quad (7)$$

Where μ_E and σ_E^2 can be reparameterised with equation (5). This intercept is approximately s_1/μ_H for a variant of small effect (s_1, s_2 and s_3 are all small). The equation for the slope of the tangent is complicated, but again assuming small-effect variant it can be approximated as:

$$slope \approx 1 + s_1 \ \mathrm{cv}_H^2 - s_2 \quad (8)$$

with the square coefficient of variation of the generation time distribution, $\mathrm{cv}_H^2 = \sigma_H^2/\mu_H^2$. Here it is assumed to be equal to $4^2/6.5^2 = 0.38$. Thus, the slope of the (r_H, r_E) relationship is close to 1, increased by the transmissibility advantage (weighted by cv_H^2), decreased by the change in mean generation time, and unaffected to the first order by the difference in standard deviation s_3. The selection coefficient is $r_E - r_H$, the vertical distance between the (r_H, r_E) relationship and the bisector.

Likelihood:

We now formulate the likelihood for the estimated growth rates across time and across regions, denoted by $\hat{r}_H$ and $\hat{r}_E$. We derive an approximation for the distribution of $\hat{r}_H$ and $\hat{r}_E$ as a function of their true values r_H and r_E and the error variances, under the assumption that these errors are normally distributed and small. The historical strains and emerging variant growth rates are estimated from daily cases and variant frequency time series, by decomposing the cases into historical and emerging variant cases. We will formalise below how the estimated growth rates are affected by the error on variant frequency which depends on $1/N$, where N is sample size, and on the error on cases number.

Between two consecutive days, denoted for simplicity days 0 and 1, the observed variables are the total number of cases denoted $\widehat{I_0}$ and $\widehat{I_1}$ and the frequency of variant $\widehat{p_0}$ and $\widehat{p_1}$. The time is now noted as an index for clarity. The observed total number of cases is:

$$\widehat{I_0} = I_0(1+\epsilon_{I,0}) \quad (9)$$

$$\widehat{I_1} = I_1(1+\epsilon_{I,1})$$

We assume that the number of cases is Poisson distributed. When the number of cases is large, the error denoted $\epsilon_{I,0}$ (for day 0) is approximately normally distributed with mean 0 and variance $1/I_0$ (and analogously for day 1). If the number of cases is distributed as a negative binomial (over-dispersed compared to the Poisson), under some conditions the normal

approximation may still be accurate and the variance of $\epsilon_{I,0}$ will be $1/[I_0\ (1-\pi)]$ where π is the success probability of the negative binomial. In other words, the cases number can be reduced to a smaller effective cases number to account for such overdispersion.

The observed logit-frequency of the variant is:

$$\widehat{lp_0} = lp_0 + \epsilon_{lp,0} \qquad (10)$$

$$\widehat{lp_1} = lp_1 + \epsilon_{lp,1}$$

where lp is a shorthand for the logit of the frequency of the variant. In the data, the frequency of the variant was estimated by running a specific PCR on a fraction on all cases and is given by a binomial frequency distribution. If the sample size is large, the error on the logit frequency $\epsilon_{lp,0}$ is approximately normally distributed within mean 0 and variance $1/(N_0\, p_0(1-p_0))$ where N_0 is the sample size at day 0 (and similarly for day 1, variance $1/(N_1\, p_1(1-p_1))$). Here again, it is possible to account for overdispersion compared to the binomial distribution, by reducing the sample size to a smaller effective number.

The observed growth rates are linked with the observed variables through the relations:

$$\hat{r}_{WT,1} = \log\,[\hat{I}_{WT,1}/\hat{I}_{WT,0}] = \log\big[\hat{I}_1(1-\hat{p}_1)\ /\ (\widehat{I_0}(1-\widehat{p_0}))\big] \qquad (11)$$

$$\hat{r}_{V,1} = \log\,[\hat{I}_{V,1}/\hat{I}_{V,0}] = \log\,[\widehat{I_1}\,\hat{p}_1\ /\ (\widehat{I_0}\,\widehat{p_0})\,]$$

Small error approximation

Replacing the observed number of cases and frequencies with the expressions above, and approximating with a first order Taylor series in the error terms, yields:

$$\hat{r}_{H,1} = r_{H,1} + \underbrace{\epsilon_{I,1} - \epsilon_{I,0}}_{\substack{\text{error on}\\ \text{case incidence}}} + \underbrace{p_0\,\epsilon_{lp,0} - p_1\epsilon_{lp,1}}_{\substack{\text{error on}\\ \text{frequency}}} \qquad (12)$$

$$\hat{r}_{E,1} = r_{E,1} + \epsilon_{I,1} - \epsilon_{I,0} - (1-p_0)\,\epsilon_{lp,0} + (1-p_1)\,\epsilon_{lp,1}$$

The first two error terms are common to both growth rates and simply express the fact that both growth rates will be inflated if the number of cases is by chance larger at time 1 than at time 0 ($\epsilon_{I,1} > \epsilon_{I,0}$). The two last terms express the fact that estimated growth rates will be modified by the error on the estimation of the frequency. For example, the growth rate of the historical strain will be inflated if by chance the error term on frequency at day 0 is greater than that at day 1 ($p_1\epsilon_{lp,1} < p_0\,\epsilon_{lp,0}$). These terms are modulated by the true frequencies p_0 and p_1.

Under the assumption that the errors on the logit frequencies and number of cases are independent and that they are also independent between day 0 and 1, the distribution of $(\hat{r}_{H,1}, \hat{r}_{E,1})$ is bivariate normal. The mean vector is:

$$(r_{H,1}, r_{E,1}).$$

The variances (diagonal of the variance-covariance matrix) are:

$$\mathrm{V}[\hat{r}_{H,1}] = \mathrm{V}[\epsilon_{I,1}] + \mathrm{V}[\epsilon_{I,0}] + {p_0}^2\mathrm{V}[\,\epsilon_{lp,0}] + {p_1}^2\,\mathrm{V}[\epsilon_{lp,1}]$$

$$= 1/I_1 + 1/I_0 + p_0/(N_0\,(1-p_0)) + p_1/(N_1\,(1-p_1))$$

$$\mathrm{V}[\hat{r}_{E,1}] = 1/I_1 + 1/I_0\ + (1-p_0)/(N_0\,p_0) + (1-p_1)/(N_1\,p_1)].$$

The covariances are:

$$\mathrm{cov}[\hat{r}_{H,1}, \hat{r}_{E,1}] = 1/I_1 + 1/I_0\ - 1/N_0 - 1/N_1.$$

The covariance between the estimated growth rates of historical and emerging strains is expected to be negative, because only a fraction of cases are assayed for the presence of the variant ($N_0 < I_0$). Indeed, the first positive term ($1/I_1 + 1/I_0$) expresses the fact that positive covariance will be created by error in cases number (for example, larger cases number will translate into higher growth rate of both historical strains and variant). The second negative term expresses the fact that the error in estimation of variant frequency will impact $\hat{r}_{H,1}$ and $\hat{r}_{E,1}$ in opposite ways. This second negative effect will be dominant.

Definition of the likelihood

Likelihood for temporal dynamics

We now formulate more generally the likelihood of observed growth rates at all days t, $\hat{r}_{H,t}, \hat{r}_{E,t}$ with $t \in [1, t_{max}]$. Across consecutive timepoints, successive estimates of $\hat{r}_{H,1}, \hat{r}_{E,1}$ will also be correlated because they share the same error terms. These cross-time covariances will be:

$$\mathrm{cov}[\hat{r}_{H,t}, \hat{r}_{H,t+1}] = \mathrm{cov}[\epsilon_{I,t} - p_t\epsilon_{lp,t}, -\epsilon_{I,t} + p_t\,\epsilon_{lp,t}]$$

$$= -\mathrm{V}[\epsilon_{I,t}] - {p_t}^2\mathrm{V}[\epsilon_{lp,t}]$$

$$= -1/I_t - p_t/(N_t\,(1-p_t))$$

$$\mathrm{cov}[\hat{r}_{E,t}, \hat{r}_{E,t+1}] = -1/I_t - (1-p_t)/(N_t\,p_t)$$

$$\mathrm{cov}[\hat{r}_{E,t}, \hat{r}_{H,t+1}] = -1/I_t + 1/N_t$$

$$\mathrm{cov}[\hat{r}_{H,t}, \hat{r}_{E,t+1}] = -1/I_t + 1/N_t$$

Finally, the likelihood for the estimated growth rates of historical strain and mutant within a region at all days is given by the density of the multivariate normal distribution:

$$P(\hat{r}_{H,1}, \hat{r}_{E,1}, \ldots, \hat{r}_{H,t_{max}}, \hat{r}_{E,t_{max}} \mid R_{H,1}, \ldots, R_{H,t_{max}}, s_1, s_2, s_3)$$

$$= f_{\boldsymbol{m},\boldsymbol{\Sigma}}\left(\hat{r}_{H,1}, \hat{r}_{E,1}, \ldots, \hat{r}_{H,t_{max}}, \hat{r}_{E,t_{max}}\right) \quad (13)$$

where $f_{\boldsymbol{m},\boldsymbol{\Sigma}}$ is the density of the multivariate normal distribution. The mean vector $\boldsymbol{m}$ is composed of the true growth rates, which depend in turn on the temporal series of true transmissibility of historical strains $R_{H,1}, \ldots, R_{H,t_{max}}$, the temporal series of true transmissibility of the variant $R_{H,1}(1+s_1), \ldots, R_{H,t_{max}}(1+s_1)$, and the distribution of the generation time of the variant characterized by s_2, s_3. The distribution of the generation time of historical strains is assumed to be known. The covariance matrix $\boldsymbol{\Sigma}$ is block-diagonal with non-zero covariances between mutant and historical strains at the same time and at consecutive time-points, as given above. The true number of cases I_t, sample size N_t, and the true variant frequencies p_t, intervene in the expressions for the variances and covariances. In practice we approximate the true number of cases and variant frequencies by their estimations, $\hat{I}_t$ and $\hat{p}_t$.

Likelihood for spatial variation

The likelihood of a series of growth rates $\hat{r}_{H,i}, \hat{r}_{E,i}$ collected in different regions or countries indexed by i is different from that for a temporal series of $\hat{r}_{H,t}, \hat{r}_{E,t}$, because there are no correlations between growth rates measured in different countries (in contrast to temporal correlations). For such data representing spatial variation in growth rates, the mean vector is composed of the true growth rates, which depend on the transmissibilities in different countries $R_{H,i}$. The covariance matrix has diagonal given by the variances:

$$\mathrm{V}\left[\hat{r}_{H,i}\right] = 1/I_{1,i} + 1/I_{0,i} + p_{0,i}/(N_{0,i}\,(1-p_{0,i})) + p_{1,i}/(N_{1,i}\,(1-p_{1,i}))$$

$$\mathrm{V}\left[\hat{r}_{E,i}\right] = 1/I_{1,i} + 1/I_{0,i} + (1-p_{0,i})/(N_{0,i}\,p_{0,i}) + \left(1-p_{1,i}\right)/(N_{1,i}\,p_{1,i})].$$

Where 0 and 1 are the consecutive timepoints at which the growth rates are measured, and the index i denotes the country. Furthermore, the covariances between growth rates of historical strains and emerging variants are:

$$\mathrm{cov}[\hat{r}_{H,i}, \hat{r}_{E,i}] = 1/I_{1,i} + 1/I_{0,i} - 1/N_{0,i} - 1/N_{1,i}.$$

All other covariances (between quantities measured in different countries) are 0.

Simulation study

Our approach relies on several approximations. First, we assume that the age-of-infection structure of the population is always at equilibrium with the current growth rate $r(t)$ even though transmission $R(t)$ changes over time. Second, we assume that errors around cases number and frequencies are small and normally distributed. We conducted a simulation study to test our ability to infer the parameters of the variant infectivity profile in spite of these approximations.

Description of the simulation model

The simulation model is as in a previous study (24) and includes time-varying transmission, arbitrary infectivity profiles, the build-up of population immunity, and detection and isolation of cases. To model transmission dynamics, we use a discretized version of the renewal equation (see also (25)) extended to two strains, historical strains and the variant. We follow the dynamics of the number of individuals infected at day t who were infected τ days ago, and have not yet been detected and isolated, called $I_H(t,\tau)$ and $I_E(t,\tau)$. The transmission dynamics are given by the system of recurrence equations:

$$I_H(t+1,0) = R_{0,H}(t)\ \underbrace{(1 - I_t^{tot}/S_0)}_{\substack{\text{population}\\ \text{immunity}}}\ \underbrace{\sum_{\tau=0}^{\infty} w_H(\tau)\, I_H(t,\tau)}_{\substack{\text{infectivity}\\ \text{profile}}} \qquad (14)$$

$$I_E(t+1,0) = R_{0,E}(t)\ (1 - I_t^{tot}/S_0)\ \sum_{\tau=0}^{\infty} w_E(\tau)\, I_E(t,\tau)$$

$$I_H(t+1,\ \tau) = I_H(t,\ \tau-1)\ \underbrace{\big(1 - c\ y(\tau-1)\big)}_{\substack{\text{case detection}\\ \text{and isolation}}}\ \forall\ \tau \geq 1$$

$$I_E(t+1,\ \tau) = I_E(t,\ \tau-1)\big(1 - c\ y(\tau-1)\big)\ \forall\ \tau \geq 1$$

The first two equations are analogous and represent transmission to new susceptible individuals giving rise to infected individuals with time since infection 0. The parameter $R_{0,H}(t)$ reflects transmission of historical strains, and is the basic reproduction number (in the absence of interventions, and when the population is fully susceptible, i.e. $I_t^{tot} = 0$). The factor $w_H(\tau)$ is the fraction of transmission that occurs at time since infection τ, where $\sum_{\tau=0}^{\infty} w_H(\tau) = 1$. Thus $w_H(\tau)$ represents the distribution of the generation time of the virus. In practice, we use a discretized version of the gamma distribution. The infectivity profile of the virus is the product of transmissibility and the generation time distribution $R_{0,H}(t)\ w_H(\tau)$. Transmission is reduced by a factor $1 - I_t^{tot}/S_0$ by population immunity, where S_0 is the initial number of susceptible

individuals in the region. Population immunity is assumed to be the same for both variants (perfect cross-protection). The variable $I_t^{tot} = \sum_{i=1}^{t}\left(I_H(i,0) + I_E(i,0)\right)$ is the total number of individuals already infected and assumed to be fully immune at time t. The instantaneous reproduction number that accounts for population immunity but not for case isolation is $R_H(t) = R_{0,H}(t)\,(1 - I_t^{tot}/S_0)$.

The third and fourth equations are analogous and represent the dynamics of individuals infected in the past. Individuals infected $\tau - 1$ days ago now have time since infection τ, provided they were not detected and isolated. An infected individual is detected with probability c, and the probability that an individual is detected at age τ (when it is detected) is given by $y(\tau)$, with $\sum_{\tau=1}^{\infty} y(\tau) = 1$. An individual who is detected is removed from the pool of individuals that contribute to further transmission of the disease. The total number of cases detected at day t is thus:

$$C_H(t) = c\sum_{\tau=0}^{\infty} y(\tau)\, I_H(t,\tau) \quad (15)$$

$$C_E(t) = c\sum_{\tau=0}^{\infty} y(\tau)\, I_E(t,\tau)$$

And the number of detected individuals who were infected τ days ago changes as:

$$C(t+1,0) = 0 \text{ (when } \tau = 0) \qquad (16)$$

$$C(t+1,\tau) = C(t,\tau-1) + c\, I(t,\tau-1)\, y(\tau-1) \;\; \forall\, \tau \geq 1$$

Parameterisation of the simulation model

We simulate the epidemiological dynamics of historical strains and variant virus. We assume that historical strains initially grow slowly, while the emerging variant initially increases in incidence faster thanks to its transmissibility advantage. Control measures are progressively strengthened, leading to control of historical strains and then the variant. Over the period considered, the variant initially increases in frequency.

We ran the simulation for 80 days. We first ran a simulation where we assumed the basic reproduction number $R_{0,H}(t)$ changed as a Brownian motion with mean 1.5 and autocorrelation 0.05, and selected a trajectory such that the mean $R_{0,t}$ over the 20 first days exceeded 1.1 and the mean over the 20 last days was below 0.9 (Figure 2). For systematic simulations designed to test the inference algorithm, we chose three scenarios for the temporal variation in $R_{0,H}(t)$: linear decline from 1.5 to 0.5, from 1.3 to 0.7, and from 1.1 to 0.9. We assumed about 9M individuals are initially susceptible (corresponding to a large European region), and an initial

number of detected cases of 4000 historical strains infections per day and 80 variant infections per day. We assumed 50% of all infection are detected (probability of detection $c = 0.5$). The time to detection is the sum of time from infection to symptom onset (distributed as log-normal with parameters 1.518, 0.472 (26)), and the time from symptom to detection (distributed as gamma with parameters shape 0.69, rate 0.31 (24,26)). We assumed the generation time of historical strains was gamma distributed with mean 6.5 days and standard deviation 4 days (2).

Inference

For inference, we tested combinations of the s_1, s_2 parameters describing how the variant differs from the historical strains in its transmissibility and mean generation time. In the terms of the simulation model parameters, $R_{0,E}(t) = R_{0,H}(t)(1 + s_1)$. The parameter s_2 affects the parameters of the gamma distribution describing $w_E(\tau)$, while $w_H(\tau)$ is gamma-distributed with mean 6.5 days and standard deviation (sd) 4 days. We assumed the variant had the same standard deviation of generation time, $s_3 = 0$. Indeed, variants affecting the sd of generation time distribution have a very small selection coefficient which makes inference of this parameter difficult. This is seen by initial exploration of the relationship between growth rates of historical strains and variant, $\hat{r}_H$ and $\hat{r}_E$ (Supplementary Figure 1).

We systematically tested our ability to infer the s_1 and s_2 parameters. We ran the simulation model for all combinations of s_1 from 0 to 0.5 in steps of 0.1 (transmissibility advantage increased from +0% to +100%), and of s_2 from -0.4 to 0.4 in steps of 0.2. We inferred the parameters s_1 and s_2 by maximum likelihood using the expression for the likelihood in equation (13).

Heuristic for the simulation study

In principle we need to infer jointly the parameters of interest $\{s_1, s_2\}$, together with the other unknown parameters $\{R_{H,1}, \dots, R_{H,t_{max}}\}$, which can be many. We used a simplified heuristic whereby we first set the parameters $\{R_{H,1}, \dots, R_{H,t_{max}}\}$ to plausible values given $\{s_1, s_2\}$, then infer the maximum likelihood parameters $\{s_1, s_2\}$ given $\{R_{H,1}, \dots, R_{H,t_{max}}\}$, and so on. We inferred maximum likelihood parameters $\{s_1, s_2\}$ using the "BFGS" (Broyden, Fletcher, Goldfarb and Shanno) method implemented in the optim function in the software R (27). In the simulation study, we iterate this procedure five times with five different starting points for $\{s_1, s_2\}$ and select the final maximum likelihood parameter set $\{s_1, s_2, R_{H,1}, \dots, R_{H,t_{max}}\}$.

To set $\{R_{H,1}, \ldots, R_{H,t_{max}}\}$ to plausible values, we used the measured growth rates with a simplified likelihood function. The simplified likelihood does not consider the full covariance structure of the multivariate normal distribution but instead only use the variances of the distribution $\mathrm{V}[\hat{r}_{H,i}]$ and $\mathrm{V}[\hat{r}_{E,i}]$ expressed above. Given $\{s_1, s_2\}$, we set the historical strains transmissibilities to:

$$R_{H,i} = \left[\frac{1}{\mathrm{V}[\hat{r}_{H,i}]}\left(1+\frac{\sigma^2}{\mu}\,\hat{r}_{H,i}\right)^{\mu^2/\sigma^2} + \frac{1}{\mathrm{V}[\hat{r}_{E,i}]}\frac{1}{1+s_1}\left(1+\frac{\sigma^2}{\mu(1+s_2)}\,\hat{r}_{E,i}\right)^{\mu^2(1+s_2)^2/\sigma^2}\right]\left(\frac{1}{\mathrm{V}[\hat{r}_{H,i}]}+\frac{1}{\mathrm{V}[\hat{r}_{E,i}]}\right)^{-1} \quad (17)$$

This equation stems from equation (2) linking growth rates with effective reproduction number. It is reparameterised in terms of μ and σ, the mean and standard deviation of the distribution of the generation time of the historical strains. It is a weighted sum of the effective reproduction number as estimated from the historical strains growth rate $\hat{r}_{H,i}$, and the effective reproduction number as estimated from the variant growth rate $\hat{r}_{E,i}$. For the latter the mean generation time is altered by $(1+s_2)$, and the transmissibility is altered by $(1+s_1)$. The weights are the inverse variance of each of the estimated growth rates, $1/\mathrm{V}[\hat{r}_{H,i}]$ and $1/\mathrm{V}[\hat{r}_{E,i}]$.

The estimated growth rate of the historical strains and variants at time *i* are given by equation (11) applied to each time-point:

$$\hat{r}_{H,i} = \log\left[\hat{I}_{i+1}(1-\hat{p}_{i+1}) \,/\, (\hat{I}_i(1-\hat{p}_i))\right] \quad (18)$$

$$\hat{r}_{E,i} = \log\left[\left(\hat{I}_{i+1}\,\hat{p}_{i+1}\right) \,/\, (\hat{I}_i\,\hat{p}_i)\right]$$

We systematically verified in the simulations that this heuristic converged to a set of $R_{H,i}$ close to the true effective reproduction number.

Full inference for analysis of English and European data

We ran inference on three datasets, two based on temporal variation in growth rates in England, and the third based on spatial variation across European countries:

(1) Data on the growth of the Alpha variant in England from 08/09/2020 to 16/03/2021. The frequency of the Alpha variant is estimated from "S-gene target failures" which reflect the deletion 69-70 in the gene S typical of Alpha.

(2) Data on the growth of the Delta variant in England from 23/03/2021 to 15/06/2021. The frequency of the Delta variant is again estimated from "S-gene target failures", where this time the "historical strains" is the Alpha variant and the Delta variant which does not have the del69-70 in gene S emerges.

(3) TESSy data from the European Centre for Disease Prevention and Control (28), on the growth of the Delta variant based on viral isolates sequenced in eleven European countries: Austria, Belgium, Denmark, France, Germany, Greece, Ireland, Italy, Netherlands, Norway, Sweden. We selected countries with sufficient data (based on visual inspection of the frequency trajectory of Delta), and used for each country the growth rates between the two weeks when the frequency of the Delta variant passed 50%.

As these datasets present a limited number of weeks or countries, it was possible to directly infer jointly the complete parameter set, $\{s_1, s_2, R_{H,1}, \dots, R_{H,t_{max}}\}$ for temporal datasets, $\{s_1, s_2, R_{H,1}, \dots, R_{H,n_c}\}$ for the spatial dataset where $n_c = 11$ is the number of countries. Furthermore, we ran optimisations for several effective number of cases and sample sizes, to select the best amount of overdispersion (Supplementary Figure 4). Each optimisation is conducted with 30 iterations of the BFGS algorithm with 30 random initial parameter values, and selecting the final best optimisation. The 95% confidence intervals on the parameters were computed assuming multivariate normality of the likelihood function, and estimating the Hessian matrix of this multivariate normal at the optimum.

671 Acknowledgements: FB was funded by a Momentum grant from CNRS. We thank Public
672 Health England and The European Surveillance System (TESSy) of the European Centre for
673 Disease Prevention and Control for sharing data on variant frequency.

674 Competing interests: none.

675

676

References

1. Volz E, Hill V, McCrone JT, Price A, Jorgensen D, O'Toole Á, et al. Evaluating the Effects of SARS-CoV-2 Spike Mutation D614G on Transmissibility and Pathogenicity. Cell. 2021 Jan 7;184(1):64-75.e11.

2. Volz E, Mishra S, Chand M, Barrett JC, Johnson R, Geidelberg L, et al. Assessing transmissibility of SARS-CoV-2 lineage B.1.1.7 in England. Nature. 2021 Mar 25;1–17.

3. Davies NG, Abbott S, Barnard RC, Jarvis CI, Kucharski AJ, Munday JD, et al. Estimated transmissibility and impact of SARS-CoV-2 lineage B.1.1.7 in England. Science [Internet]. 2021 Apr 9 [cited 2021 Apr 16];372(6538). Available from: https://science.sciencemag.org/content/372/6538/eabg3055

4. Borges V, Sousa C, Menezes L, Gonçalves AM, Picão M, Almeida JP, et al. Tracking SARS-CoV-2 VOC 202012/01 (lineage B. 1.1. 7) dissemination in Portugal: insights from nationwide RT-PCR Spike gene drop out data. Virol Org. 2021;

5. Washington NL, Gangavarapu K, Zeller M, Bolze A, Cirulli ET, Schiabor Barrett KM, et al. Emergence and rapid transmission of SARS-CoV-2 B.1.1.7 in the United States. Cell [Internet]. 2021 Mar 30 [cited 2021 Apr 16]; Available from: https://www.sciencedirect.com/science/article/pii/S0092867421003834

6. Gaymard A, Bosetti P, Feri A, Destras G, Enouf V, Andronico A, et al. Early assessment of diffusion and possible expansion of SARS-CoV-2 Lineage 20I/501Y.V1 (B.1.1.7, variant of concern 202012/01) in France, January to March 2021. Eurosurveillance. 2021 Mar 4;26(9):2100133.

7. Campbell F, Archer B, Laurenson-Schafer H, Jinnai Y, Konings F, Batra N, et al. Increased transmissibility and global spread of SARS-CoV-2 variants of concern as at June 2021. Eurosurveillance. 2021 Jun 17;26(24):2100509.

8. Wallinga J, Lipsitch M. How generation intervals shape the relationship between growth rates and reproductive numbers. Proc R Soc B Biol Sci. 2007 Feb 22;274(1609):599–604.

9. Park SW, Bolker BM, Funk S, Metcalf CJE, Weitz JS, Grenfell BT, et al. Roles of generation-interval distributions in shaping relative epidemic strength, speed, and control of new SARS-CoV-2 variants. medRxiv. 2021 May 5;2021.05.03.21256545.

10. Public Health England. SARS-CoV-2 variants of concern and variants under investigation Technical Briefing 9 [Internet]. Public Health Engalnd; [cited 2021 Jun 21]. Report No.: 9. Available from: https://assets.publishing.service.gov.uk/government/uploads/system/uploads/attachment_data/file/979818/Variants_of_Concern_VOC_Technical_Briefing_9_England.pdf

11. Public Health England. SARS-CoV-2 variants of concern and variants under investigation Technical Briefing 17 [Internet]. Public Health Engalnd; [cited 2021 Jun 21]. Report No.: 17. Available from:

https://assets.publishing.service.gov.uk/government/uploads/system/uploads/attachment_data/file/1001354/Variants_of_Concern_VOC_Technical_Briefing_17.pdf

12. Kissler SM, Fauver JR, Mack C, Tai CG, Breban MI, Watkins AE, et al. Viral dynamics of SARS-CoV-2 variants in vaccinated and unvaccinated individuals [Internet]. 2021 Aug [cited 2021 Sep 25] p. 2021.02.16.21251535. Available from: https://www.medrxiv.org/content/10.1101/2021.02.16.21251535v3

13. Cosentino G, Bernard M, Ambroise J, Giannoli J-M, Guedj J, Débarre F, et al. SARS-CoV-2 viral dynamics in infections with variants of concern in the French community [Internet]. 2021 [cited 2021 May 18]. Available from: https://hal.sorbonne-universite.fr/hal-03217231

14. Elie B, Lecorche E, Sofonea MT, Trombert-Paolantoni S, Foulongne V, Guedj J, et al. Inferring SARS-CoV-2 variant within-host kinetics [Internet]. 2021 May [cited 2021 Sep 25] p. 2021.05.26.21257835. Available from: https://www.medrxiv.org/content/10.1101/2021.05.26.21257835v1

15. Zhang M, Xiao J, Deng A, Zhang Y, Zhuang Y, Hu T, et al. Transmission Dynamics of an Outbreak of the COVID-19 Delta Variant B.1.617.2 — Guangdong Province, China, May–June 2021. China CDC Wkly. 2021 Jul 2;3(27):584–6.

16. Pung R, Mak TM, Group CC-19 working, Kucharski AJ, Lee VJ. Serial intervals observed in SARS-CoV-2 B.1.617.2 variant cases. medRxiv. 2021 Jun 4;2021.06.04.21258205.

17. Ryu S, Kim D, Lim J-S, Ali ST, Cowling BJ. Serial interval and transmission dynamics during the SARS-CoV-2 Delta variant predominance in South Korea [Internet]. 2021 Oct [cited 2021 Oct 27] p. 2021.08.18.21262166. Available from: https://www.medrxiv.org/content/10.1101/2021.08.18.21262166v2

18. Alizon S, Haim-Boukobza S, Foulongne V, Verdurme L, Trombert-Paolantoni S, Lecorche E, et al. Rapid spread of the SARS-CoV-2 δ variant in the area of Paris (France) in June 2021. medRxiv. 2021 Jun 20;2021.06.16.21259052.

19. Blanquart F, Abad C, Ambroise J, Bernard M, Cosentino G, Giannoli J-M, et al. Spread of the Delta variant, vaccine effectiveness against PCR-detected infections and within-host viral load dynamics in the community in France [Internet]. 2021 [cited 2021 Jul 21]. Available from: https://hal.archives-ouvertes.fr/hal-03289443

20. Roquebert B, Trombert-Paolantoni S, Haim-Boukobza S, Lecorche E, Verdurme L, Foulongne V, et al. The SARS-CoV-2 B.1.351 lineage (VOC β) is outgrowing the B.1.1.7 lineage (VOC α) in some French regions in April 2021. Eurosurveillance. 2021 Jun 10;26(23):2100447.

21. Kraemer MUG, Pybus OG, Fraser C, Cauchemez S, Rambaut A, Cowling BJ. Monitoring key epidemiological parameters of SARS-CoV-2 transmission. Nat Med. 2021 Nov 8;1–2.

22. Roquebert B, Haim-Boukobza S, Trombert-Paolantoni S, Lecorche E, Verdurme L, Foulongne V, et al. SARS-CoV-2 variants of concern are associated with lower RT-

PCR amplification cycles between January and March 2021 in France. medRxiv. 2021 Mar 22;2021.03.19.21253971.

23. Public Health England. SARS-CoV-2 variants of concern and variants under investigation in England. Technical Briefing 16 [Internet]. 2021 Jun [cited 2021 Jun 28]. Available from: https://assets.publishing.service.gov.uk/government/uploads/system/uploads/attachment_data/file/994997/Variants_of_Concern_VOC_Technical_Briefing_16.pdf

24. Belloir A, Blanquart F. Estimating the global reduction in transmission and rise in detection capacity of the novel coronavirus SARS-CoV-2 in early 2020. Epidemics. 2021 Jun 1;35:100445.

25. Flaxman S, Mishra S, Gandy A, Unwin HJT, Mellan TA, Coupland H, et al. Estimating the effects of non-pharmaceutical interventions on COVID-19 in Europe. Nature. 2020 Jun 8;1–8.

26. Lauer SA, Grantz KH, Bi Q, Jones FK, Zheng Q, Meredith HR, et al. The Incubation Period of Coronavirus Disease 2019 (COVID-19) From Publicly Reported Confirmed Cases: Estimation and Application. Ann Intern Med. 2020 Mar 10;172(9):577–82.

27. R Core Team. R: A Language and Environment for Statistical Computing. Vienna, Austria: R Foundation for Statistical Computing; 2018.

28. Data on SARS-CoV-2 variants in the EU/EEA [Internet]. European Centre for Disease Prevention and Control. 2021 [cited 2021 Sep 24]. Available from: https://www.ecdc.europa.eu/en/publications-data/data-virus-variants-covid-19-eueea

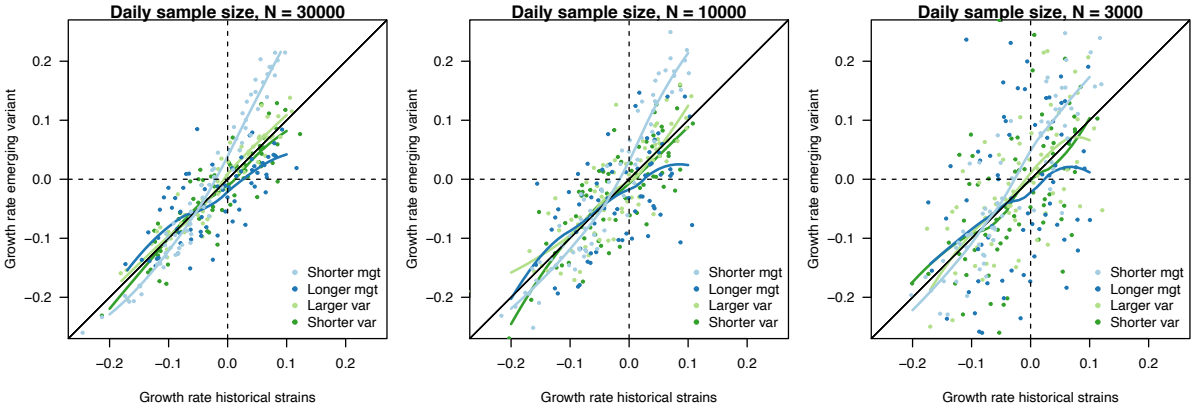

Supplementary Figure 1: The relationship between estimated growth rate of the variant and historical strains across time in the simulation study, in the scenario of progressive decline of $R_{0,H}(t)$ from 1.5 to 0.5. The three panels are three daily sample sizes to assess variant frequency (30000, 10000, 3000). This is shown for variants with no transmissibility advantage $s_1 = 0.$, and four scenarios of infectivity profiles: shorter mean generation time ($s_2 = -0.4, s_3 = 0$), longer mean generation time ($s_2 = +0.4, s_3 = 0$), larger sd ($s_2 = 0, s_3 = +0.4$) and smaller sd ($s_2 = 0,\ s_3 = -0.4$). Points are the estimated growth rates with error, the curves show local polynomial regression (loess). The selection coefficient is the vertical distance to the bisector. A variant with a shorter mean generation time presents a steeper relationship between the two growth rates (light blue curve), meaning that the selection coefficient is maximal when transmission is large (fast growing epidemic) (Figure 1C, D). On the contrary, a variant with a longer generation time presents a flatter relationship (dark blue curve), with selection coefficient being maximal when transmission is small. This distinction blurs when the number of cases sampled to assess variant frequency decreases. Variants changing the variance of the distribution (green curves) appear almost neutral, with curves close to the bisector.

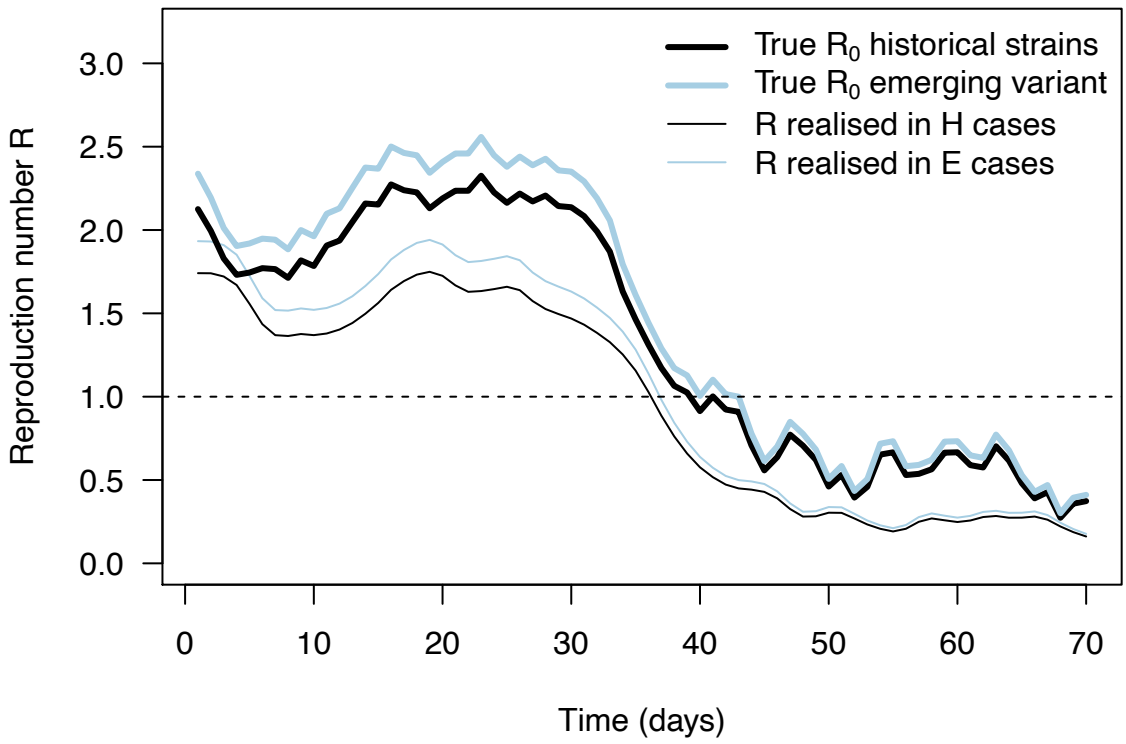

795

796 **Supplementary Figure 2:** The daily basic reproduction number of the historical strains and variant ($R_{0,H}(t)$ and
797 $R_{0,E}(t)$, identical thick lines), together with the effective reproduction number inferred from daily case and
798 frequency data (thin lines), in the example simulation shown on Figure 2B for an emerging variant with +10%
799 effective reproduction number and same distribution of generation time. These realized effective reproduction
800 number present a trend similar to the true basic reproduction number inputted to the simulation with three
801 differences. First, the realized effective reproduction number are shifted in time compared to $R_{0,H}(t)$ because of
802 the time shift between infections and case detection. Second, the realized effective reproduction number is lower
803 than the true $R_{0,H}(t)$ because of population immunity and case detection and isolation. Third, error in cases
804 numbers and in variant frequency cause error in the inferred effective reproduction number.

805

806

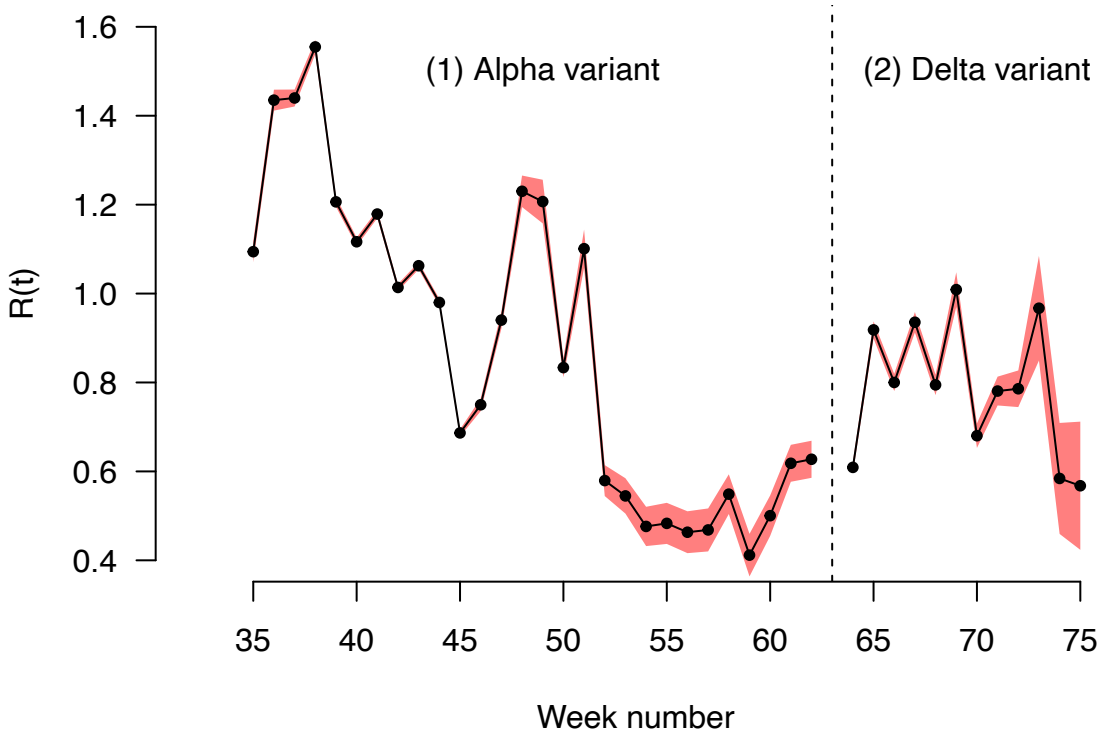

807

808 **Supplementary Figure 3:** The effective reproduction number of historical strains $R_H(t)$ estimated on the English
809 data, for the period when the Alpha variant emerged and replaced historical strains, then the period when the Delta
810 variant emerged and replaced the Alpha variant and other strains. The two periods are separated by the dashed
811 vertical line. Black points show the maximum likelihood estimates, red shaded areas the 95% confidence interval.

812

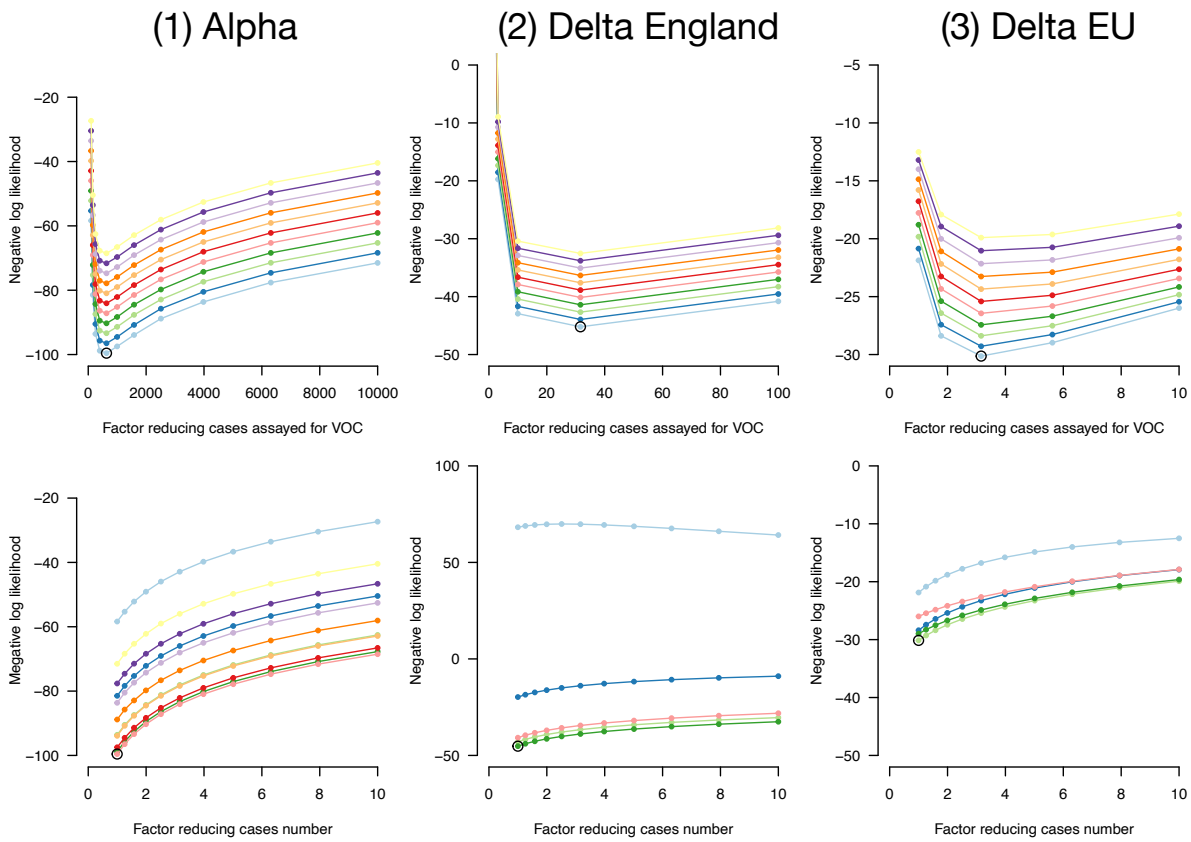

Supplementary Figure 4: Negative log-likelihood of the fully optimised model as a function of overdispersion in number of cases and in emerging variant frequency. Overdispersion is represented by two factors: a factor reducing the number of cases, thus increasing the variance of the error in cases number compared to a Poisson, and a factor reducing the sample size, thus increasing the variance in frequency compared to a binomial. We optimised likelihood for all combinations of the two factors. Top panels, negative likelihood of the optimised model as function of the factor reducing the number of cases. Bottom panels, as a function of the factor reducing the sample size. The best combination of factors is highlighted as an open point. This is shown for the three datasets (left, middle, right columns).